

Toward a Dynamic Vertical Climbing Robot

Jonathan E. Clark¹, Daniel I. Goldman², Tao S. Chen², Robert J. Full², and Daniel Koditschek¹

¹GRASP Laboratory, University of Pennsylvania

Department of Electrical and Systems Engineering
200 S. 33rd Street, Philadelphia, PA, USA

²PolyPedal Laboratory, Department of Integrative Biology
University of California at Berkeley, Berkeley, CA 94720, USA
email: jonclark@seas.upenn.edu

Abstract—

Simple mathematical models or ‘templates’ of locomotion have been effective tools in understanding how animals move and have inspired and guided the design of robots that emulate those behaviors. This paper describes a recently proposed biologically-based template for dynamic vertical climbing, and evaluates the feasibility of adapting it to build a vertical ‘running’ robot.

We present the results a simulation study suggesting that appropriate mechanical and control alterations to the template result in fast stable climbing that preserves the characteristic body motions and foot forces found in the template model and in animals. These design changes should also allow the robot to operate with commercially available actuators and in the same power to weight range as other running and climbing robots.

I. INTRODUCTION

Vertical climbing robots, much like their horizontal walking counterparts, have traditionally been restricted to slow, quasi-static gaits on benign surfaces. For cursorial robots the era of fast, dynamic robots began with the hopping machines pioneered by Raibert and his colleagues in the early 80s. The motions and ground reaction forces of these robots, as well as those of a wide range of animals, can be characterized by the Spring-loaded Inverted Pendulum (SLIP) model [1], [2], [3], [4]. This simple planar model has been used for inspiration and guidance in the design and development of a number of recent polypedal robots, such as RHex [5] and Sprawl [6], that are capable of fast (multiple body-lengths/second) locomotion even over rough and broken terrain.

These robots actively manage their kinetic energy during running by using spring/dampers in series with their motors. They have a limited number of powerful actuators and run primarily open loop, simplifying their control. Stable operation is provided by appropriate tuning of the passive elements.

Thus far, vertically climbing robots have lacked such an enabling template to guide their development. Until recently most climbing robots have relied upon suction or electromagnets to achieve the required adhesive foot forces [7], [8]. More recently some robots have been developed that use foot-holds [9], [10] or vectored thrust [11], [12] to cling to walls. The last few years have also seen the revival [13], [14] of a design introduced by [15] that used rimless wheels with sticky toes to intermittently ‘roll’ up smooth walls.

Another recent biologically inspired legged robot, RiSE, has been developed that uses claws, micro-spines,

and dry adhesives to extend its range of traversable vertical surfaces to include rough man-made and natural terrain [16].

While these developments entail significant advances in attachment mechanisms and the control strategies that derive advantage from them, the agility and speed of these climbers pales in comparison to their biological counterparts. Geckos can climb walls at speeds of up to 0.77 m/s [17] and cockroaches have been measured to climb at five body-lengths per second [18]. Recent comparative biological studies suggest compelling similarities between animals with vastly different morphologies and attachment mechanisms. The emergence of these patterns has led to a proposed two-legged dynamic template for climbing (Fig. 2) [18]. It is this model that we use to guide the development of what may be the world’s first dynamic legged vertical climber.

Animals, however, enjoy roughly an order of magnitude greater power density relative to commercially available actuators [19] and the question arises whether this dramatic advantage places their dynamical climbing strategies out of reach of contemporary robotics. In this paper, we introduce the preliminary design of a simple robotic ‘anchor’ for the proposed animal climbing template (Fig 9). This prototype design features the sprawled posture and series springs characteristic of the template, but adopts a scale (from 2g to 2kg) and mass distribution closer to the RiSE robot to better enforce engineering constraints. We evaluate the effectiveness of adding parallel leg springs and a force-based control strategy as proposed in [20] to replace the template’s clock driven feed forward limb trajectories in compensation for the dramatically reduced power budget.

This paper describes the conclusions of a simulation study designed to guide the physical construction of the robotic anchor, and is organized as follows: Section II introduces the template model and describes how it was developed from animal studies. In section III we scale the template model to our target robot mass, and evaluate the effect of the changes in length, stiffness, and frequency on the locomotion dynamics. Section IV compares the power consumption of this scaled template to the range of the best commercial off-the-shelf actuators. Here we attempt to answer the question: with a limited power budget what happens to the dynamics of locomotion? In section VI, we apply some of the techniques from our 1 DOF numerical study on climbing to make more efficient use of the available motor

power and describe the effect of these changes on the resulting dynamics. We conclude by describing a proposed robot morphology and some of the issues associated with translating our model into three dimensions.

II. TEMPLATE MODEL

The recent biomechanical analysis of the rapid vertical climbing of the cockroach *Blaberus discoidalis* shows striking similarities to early studies of geckos running up walls. Although these animals are from distinct phyla (Arthropoda and Chordata) and have a different number of legs, body morphology, and attachment mechanisms, their locomotion patterns (see Fig. 1 A&B) are strikingly similar. They both create large lateral in-pulling forces with their legs, and their center of mass velocities are phase delayed from the forces by approximately $\pi/2$. These similarities have led to the development of a proposed dynamic climbing template shown in Fig. 2 and detailed in [18].

This proposed template model features a pair of virtual legs rigidly attached to the body that alternate in pulling the robot upwards. The inclusion of a lateral sprawl angle β in the model helps create the characteristic lateral forces, and appears to contribute significantly to the climbers rotational stability [18]. Each leg also features a spring/damper in series with the sinusoidally oscillating leg actuators. These springs reduce the peak wall reaction force felt by the feet, and affect the phasing of the motions. In this model the actuator is commanded to follow a sinusoidal trajectory and the foot contact is modeled as a pin joint with an attachment duty factor of 46%. With the actuation scheme and parameter set specified in Fig. 2, the template climbs at 18 *cm/s* and with force and velocity patterns similar to the animals that inspired it (see Fig. 1C).

III. SCALING OF TEMPLATE

The first task in evaluating the viability of this template as a basis for RiSE-scale robot design is to devise a scaling method that preserves its dynamics in a regime with at least two and possibly three orders of magnitude greater mass.

A. Scaling Rules

The motivation behind the particular set of scaling rules employed here is to preserve the dynamic similarity of the system, in particular the relative frequencies of the body pendulum, the wrist-spring, and the overall leg actuation frequency. If dynamic similarity is preserved then all of the resulting displacements, times, and forces are scaled versions of the original [21], and the stability characteristics are invariant. [22]. A more detailed discussion of dynamic similarity and a derivation of the associated scaling laws adapted below is given in [23].

All linear dimensions of the body were scaled geometrically by (α_L) which in our case equals 10. Mass was assumed to scale as the cube of length, the total mass of the robot increasing by $(\alpha_L)^3$ from 2g to 2kg. Similarly the rotational inertia was increased by $(\alpha_L)^5$.

In order to sustain the relationship between body oscillation and foot alternation, the gait driving frequency was scaled down to match the longer period of a pendulous body oscillating about the pinned stance foot. Since this pendular frequency is proportional to $\sqrt{g/l}$, the leg actuation frequency scale factor (α_ω) was defined to be:

$$\alpha_\omega := \sqrt{\frac{1}{\alpha_L}} = 0.316$$

This results in the driving frequency changing from 9 Hz to 2.85 Hz.

The stiffness of the wrist springs was scaled such that the maximum force exerted by the spring at full deflection matched the increased weight of the body $F = mg = kx$. Consequently the stiffness scale factor (α_k) is:

$$\alpha_k := \frac{\alpha_L^3}{\alpha_L} = 100$$

This also preserves the relative frequency of the wrist spring-body oscillation, $\omega_{spring} = \sqrt{k/m}$, such that:

$$\alpha_k := (\alpha_\omega)^2 \cdot (\alpha_L)^3 = 100$$

In fact, this scaling approach results in a constant Strouhal Number (*Str*):

$$Str := \frac{\omega l}{V}$$

which it has been argued is necessary for any spring-based or cyclic scaling system that preserves dynamic similarity [23].

Since the overall velocity of the scaled climber is based on the speed of the leg actuator, the scaled robot velocity (*V*) should be:

$$\alpha_V := \alpha_\omega \cdot \alpha_L = 3.16$$

This method of scaling preserves the non-dimensional Froude number (*Fr*) used by some researchers [24], [25] to characterize scale independent running speed.

$$Fr := \frac{V}{\sqrt{gl}}$$

In consequence of dynamic similarity, the resulting Froude number is precisely same for both the template and the scaled version of the climber [23]. Note however, if we calculate speed using the body-lengths per second (bl/s) metric, the template climbs at 4.5 bl/s, and the scaled version at only 1.4 bl/s. This reveals the under-determined nature of the Froude number as a basis for speed comparison between different robotic designs: there is still a design decision to be made regarding the characteristic length, *l*. It is often described as the ‘leg length’ or the distance from the hip to the foot, however it is not clear that this convention has the same effect in upright as in sprawled posture runners. For example, in our climber if the stroke length of the actuator is used as the characteristic leg length

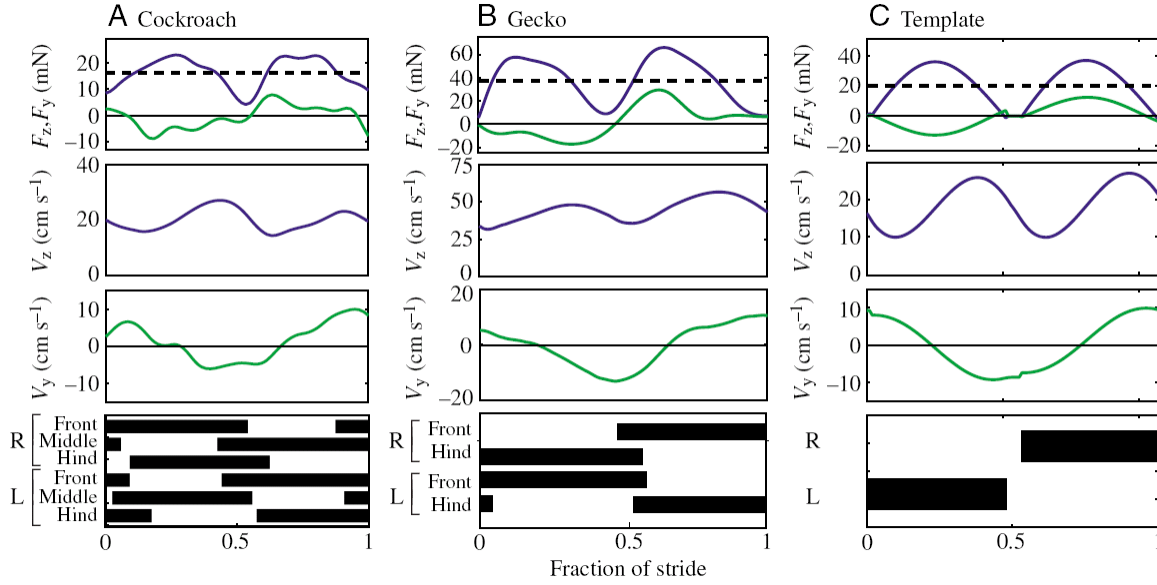


Fig. 1. Force, vertical velocity, lateral velocity, and foot fall patterns for the cockroach, gecko, and template model. Broken lines indicate body weight. Data are shown for a normalized stride, with black bars representing foot contact. In each force plot F_z is the magnitude in the vertical direction and F_y is in lateral direction. Reproduced with permission from [18]

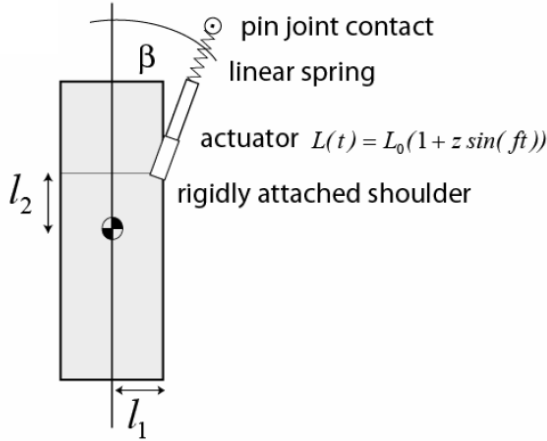


Fig. 2. Diagram of the two degree of freedom climbing template. The spring acts in series with the sinusoidal linear actuator. The model was built and integrated in Working Model 2D (Design Simulation Technologies, Inc). The parameters used to generate Fig. 1C were: body mass = 2 g, body dimensions = 4 cm x 0.95 cm, $l_1 = 0.71$ cm, $l_2 = 0.84$ cm, $\beta = 10^\circ$, $L_0 = 1.54$ cm, actuator fractional length change $z = 0.6$, stiffness $k = 6$ Nm $^{-1}$, damping $\gamma = 0.09$ Nsm $^{-1}$, frequency $f = 9$ Hz. Moment of inertia = 8×10^{-7} kgm 2 . The attachment duty factor in the model is 0.46. Adapted from [18].

then the template and scaled climber have a characteristic speed of 0.73, if the length from the ‘hip’ to the foot is utilized, the Froude number becomes 0.45, and if the body height is used it drops to 0.28. Perhaps the intermediary value would be most appropriate, but regardless of which length is chosen the Froude number remains invariant to scale as long as the motions are dynamically similar.

The damping in the wrist spring was also scaled such the the force exerted by the damper balances the increased mass and decreased velocity of the climber $F = mg = b \cdot V$, such that:

$$\alpha_b := \frac{\alpha_L^3}{\alpha_V} = 316$$

B. Comparison of Scaled Template

Figure 3 presents a typical simulation output in the steady state regime illustrating the effects of increased size on template behavior under the scaling model proposed above. The overall speed of the scaled template (both laterally and vertically) is just over three times faster, as expected. The wall reaction forces generated by this larger version of the template are also three orders of magnitude larger, again, as expected. It appears that the phasing of the motions and forces and the regular oscillatory pattern have also been preserved.

C. Scaling and Power

Biological actuators (muscles) differ from and are in many ways superior to current commercially available power generators. A nice overview of the properties of and physics behind a variety of possible robotic actuators is given in [26]. For the purpose of this paper, we

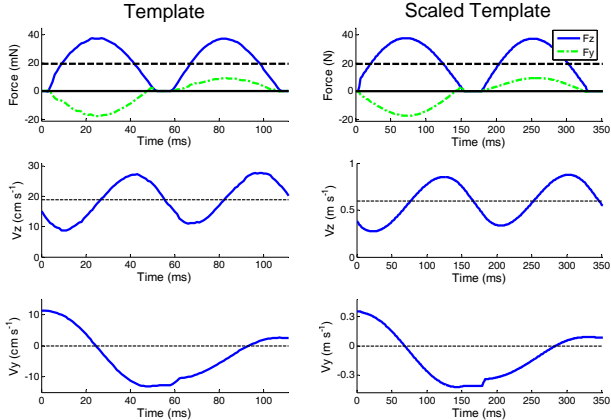


Fig. 3. Force, vertical velocity, and lateral velocity for the template model and the robot scaled version. The heavy dashed horizontal lines represent the weight of the robot and the light dashed lines are the mean velocities.

will restrict ourselves to DC motors, and assume that their power scales directly with mass. This presents the major problem in scaling up a dynamic system. When we increase the length by a factor of 10, we also increase the needed power to weight ratio by:

$$\frac{\Delta power}{\Delta weight} = \frac{F \cdot V}{mg} = \frac{\alpha_L^3 \cdot \alpha_V}{\alpha_L^3} = 3.16$$

Since the power density of actuators does not increase with mass, it becomes more difficult to provide the power necessary to achieve the template-based dynamics as our scale increases.

The historically achievable power density of climbing and running robots varies greatly, but as a point of reference both the hexapedal RiSE and RHex robots have a specific power of about 10W/kg per tripod. The template model, at the roach scale, requires a peak of 6.3W/kg per leg. However, scaling to a 2kg climber increases this power demand by 3.16 to 20W/kg per leg. Thus the model requires the availability of twice as much peak power from the motors as has been available in these previous robotic designs.

Consequently, at the scale of interest we are required to either dramatically increase the power density of our robots, find a method to deliver the power much more efficiently, or settle for slower speeds. Assuming that the power density in a robot with a significant computational payload is relatively inflexible, we proceed in the next section to discuss the effects of reducing the available input power on the dynamics, and then consider ways to optimize available power.

IV. POWER LIMITATIONS

There are a number of possible methods for reconciling the difference between desired and available power. We will first consider the two simplest strategies: reducing the actuation frequency and reducing the required actuator force by shortening the crank moment arm. In

each case the naive expectation is that the net result will be climbing speeds that are one half of the nominal case.

The potential problem with altering the actuation frequency is that it will disrupt the dynamics of climbing by producing a detrimental interaction with the body's natural dynamics. Simulations show that decreasing the stride frequency by a factor of two does result in stable motions, but there is much greater body swing during each stride. This dramatically increases the lateral forces seen at the feet, and lateral velocity of the robot, as shown in Fig. 4A. This larger rotation reduces the vertical component of each stride, dramatically (over 10x) reducing the upward speed of the climber. Peak required power is reduced from 40W to 23W.

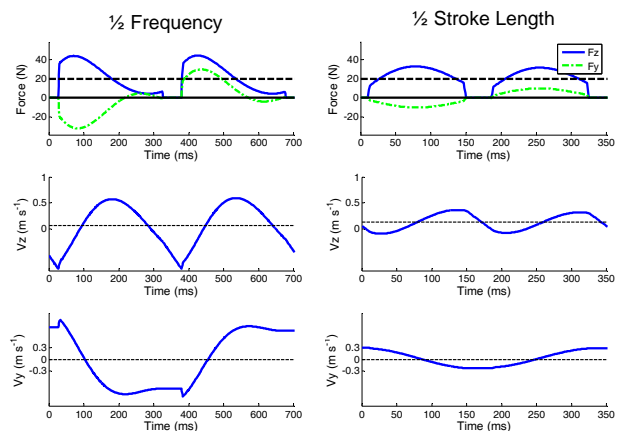


Fig. 4. Force, vertical and lateral velocity for two simple approaches to reducing the power of the scaled template model. Note that the tick marks for force and velocity have been preserved from Fig. 3 to ease comparison.

The second simple strategy, cutting the stride length in half by shortening the crank, does change the pendular frequency of the body slightly, but this does not seem to significantly affect the stability of the gait. As shown in Fig. 4B, the forces and velocities of the climber with a reduced crank length are essentially the same as in the nominal case with the exception of slightly larger lateral forces. The net vertical velocity is, however, reduced to 20-25% of the scaled template's speed. The deterioration of upward velocity is exacerbated by the increased slip due to the sub 50% duty factor prescribed by the attachment strategy. The peak power, however, is reduced to 18W.

In both cases we see that using these simple approaches to reducing the peak power required from the actuator result in serious compromises in the performance of the template. There are, of course, other methods to deal with limited actuator power.

One such method is the intermittent use of the motors at speeds and loads exceeding their limits for recommended continuous use. For short periods the motors can be 'overrun', but this produces more heat than can be effectively dissipated, resulting in eventual overheat-

ing of the motors—unless the power draw is subsequently decreased. This ‘thermal borrowing’ can be used for short periods if mean power draw is low enough. This has been successfully used in RHex for rough terrain, stair climbing, etc. but only for very limited durations. In vertical climbing, however, the high power demand is constant. Nevertheless this approach allows us to exceed the specified maximum continuous torque levels, if only for short segments of the cycle.

Another approach to decreasing the total required motor power is to mechanically couple multiple joints or limbs to be driven by a single motor. This technique has been employed by iSprawl[27], MechaRoach [28], and several toy robots. This approach, however, prescribes rigidly fixed leg synchronization, which in climbing can be a serious problem. In addition, this would further hinder any future development into a more versatile runner/climber.

There are two additional ideas for dealing with a limited power budget suggested in [20]. The application of these to the scaled template will be discussed in section VI. Before proceeding with that discussion it is necessary to address some implementation and modeling issues for the robot and actuator.

V. MASS DISTRIBUTION AND LINKAGE DESIGN

Due to geometric constraints associated with magnetics and electromechanics, it is possible to build rotary motors with much higher power densities than linear motors. If standard rotary motors are to be used on the robot, the question then arises how to convert the output of a real DC motor into the linear motion prescribed by the climbing template. The approach we have taken is to utilize a simple crank-slider mechanism (similar to the piston/crank used in automobile engines), as shown in Fig. 5. Thus the transformation from linear to rotational coordinates is specified by the geometry of the mechanism.

To account for the need to have a mechanism to attach/detach from the wall, and the necessary strength of the crank-slider mechanism, we have distributed some of the mass (as shown in Fig. 5) of the robot from the body to the legs. The total mass and length of the climber, has, however remained unchanged.

This addition of mass to the rotating links does introduce some added dynamics to the system. The more massive the cranks, the more energy can be stored in this part of the system (as a small fly-wheel) helping to smooth out the resulting motions of the legs. The simulation suggests, however, that the results of the next section hold, even with a less-favorable mass distribution than that shown above.

In addition, a degree of freedom and lateral compliance have been added to each of the hips. This removes the kinematic singularity associated with double support phase. The stiffness and damping of the hips are set equal in magnitude to the wrist springs, but since they are typically orthogonal to gravity, their deflection primarily occurs when both legs are attempting to

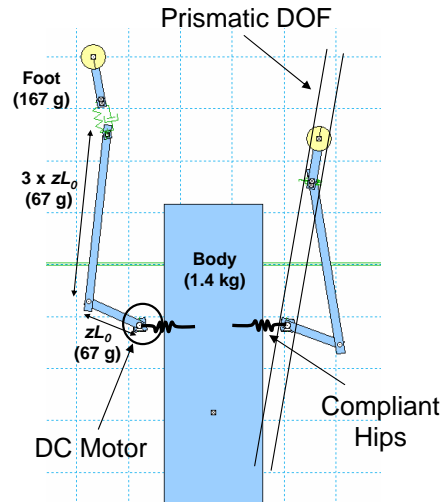


Fig. 5. Schematic of the crank-slider mechanism used to convert rotary (motor) output into linear motion. The relative lengths and masses of the links are indicated.

simultaneously contract during double support.

The results of switching to the crank-slider morphology with realistic leg masses is that the peak speed is reduced to 0.53 m/s and the peak power is 35 W , as compared to 0.56 m/s and 40 W for scaled template. The dynamics are nearly the same as for the scaled template, and are shown in Fig. 8A.

VI. SPRINGS AND FORCE BASED CONTROL

A. Parallel springs

One way to assist climbing with a limited power budget is using passive-elastic elements in parallel with the leg actuators to store energy during the swing-recirculation phase of the leg motion, and then to release the energy during stance to aid with accelerating the body upwards.

As suggested in [20] this can substantially increase the overall climbing speed of a one-dimensional climber by creating a second peak in the demanded power curve for each motor. Figure 6 shows a schematic of how the spring is used, and a plot of motor power as a function of time. The shaded areas represent the changes in the commanded torque with the addition of a spring in parallel with the actuator connecting each foot to the body.

The spring is at its unloaded, or rest, position when the foot is at its lowest position. As the foot extends in preparation for reattachment to the substrate the spring is stretched, significantly increasing the torque required from the actuator. The maximum available motor torque, and the length of the crank linkage define the upper limit on the stiffness of this spring.

With the addition of these legs springs ($k=130 \text{ N/m}$, $b=3 \text{ N-s/m}$) the peak power required for each legs drops to 25 W during steady state climbing. Since the velocity of the cranks is still constant, the dynamics of the

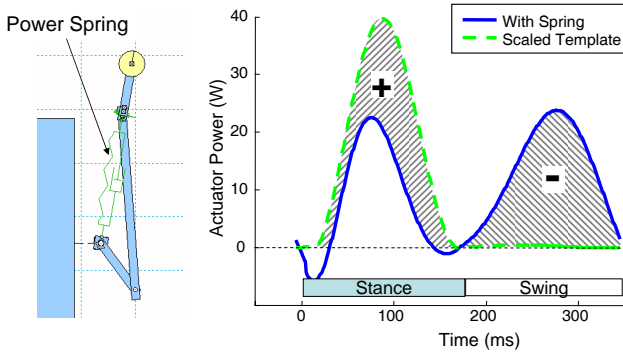


Fig. 6. Schematic of model with leg spring and the effect of the spring on the nominal torque profile. The ‘+’ region represents the effect of the spring assisting the motor, and the ‘-’ region is when the motor is stretching the spring.

system are the same as without the spring.

One problem that the addition of springs in parallel with the actuator does not address is that over 40W of power are still required to accelerate the robot from rest. After the first few strides the power requirement drops to an almost-achievable level. Even though the maximum, or stall, torque that motors can produce is often more than twice that available for continuous operation, this value can only be delivered at very low speeds. Thus, the use of a real 20W motor in the initial transient stage of operation would fail to follow the prescribed trajectory either stalling or introducing a significant limb coordination problem.

B. Force Maximization Control

A second approach to increasing the use of a robot’s on-board power is to switch from a position-based control scheme to forced-based approach. By explicitly regulating the motors’ output rather than relying on position tracking errors, the actuators could be much more effectively utilized during a stride. This control framework also enables the robot to build up speed over a number of strides, further increasing the performance gains.

The feasibility of using a ‘force-maximizing’ control scheme to actuate the robot was tested in the one-degree of freedom numeric simulation in [20]. The results from this one-dimensional numeric study suggest that the appropriate addition of a force-based controller and leg springs could double the robot’s speed, and that climbing at about 2 bl/s should be achievable.

The use of this scheme also allows for the frequency of the legs to fluctuate, helping to solve the problem of large transient forces required at the initial start up.

B.1 Motor model

In order to maximize the output power of the motors, a model of their behavior must be incorporated into the control scheme. Fig. 7 depicts the simple model used in our controller. The slope of the torque/speed

curve depends on the particular motor chosen, and on the resulting gear reduction ratio used in the power train.

For our model we used the specified values for Maxon 20W DC motors [29]. The gear box reduction ($G = 48$) was chosen to match the template dynamics and maximize speed.

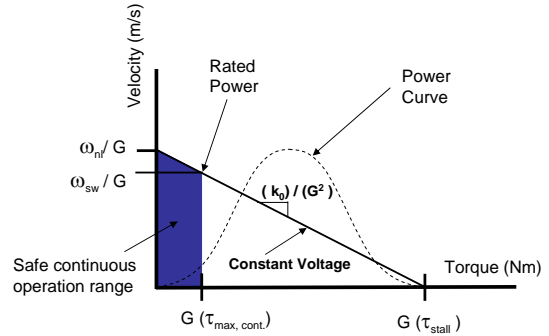


Fig. 7. Simplified geared motor model based on data from Maxon motors. The dashed power curve shows that maximum power output corresponds to loads equal to one half of stall.

The controller varies applied current/torque so that the operation point stays on the boundary of the shaded continuous operation zone shown in Fig. 7. Thus the applied torque from the motor is given by:

$$\tau = \min \left(\tau_{max,c}, \left(1 - \frac{\omega}{\omega_{nl}/G} \right) G \tau_{stall} \right)$$

It should be noted that the introduction of this motor model provides a serious constraint on both the maximum power deliver by the motor and on the achievable speeds/torques. Thus in the simulations no ‘thermal borrowing’ is allowed.

B.2 Leg coordination

A new issue arising from the introduction of the force-maximization controller is the challenge of ensuring the proper anti-phase coordination of legs. An earlier analytical study of coupled oscillatory climbing systems has shown that the limbs of these systems naturally phase lock, resulting in extremely large double support and aerial phases [30]. Our two-dimensional model exhibits the same tendency, with potentially catastrophic consequence for a physical climbing machine machine whose attachment mechanics are likely to preclude recovery from conditions of free-fall [31], [32]. Consequently some sort of mechanism is require to ensure proper phasing of the legs. We are in the process of adapting the formal phase regulation scheme of [33] to the new situation of coupled oscillators for generating reference limit cycles in the presence of forbidden obstacles (double flight phases). Temporarily, a braking heuristic is implemented to help prevent double support, and is given by:

$$\text{if}((\theta_i < \epsilon) \text{ and } (\theta_j < \pi)) \text{ then } \tau_i = -c_b \tau_{max}$$

Where ϵ is about $\pi/10$, and gait transitions occur when the leg phase angle $\theta = \pi$. This attempts to ensure a nominal duty cycle of less than 50%. In the template model a duty factor of 46% is enforced.

The solution described above is somewhat ‘brittle’. The value for (c_b) is empirically chosen, and results in unstable climbing, and a change in the actuator model or system dynamics could easily result in either extended duty factors, or significant aerial phases. It is also sub-optimal in terms of performance since it actively brakes just before stride transitions, rather than appropriately reducing the input energy throughout the swing phase.

Another problem with this approach is that it often results in a very slight asymmetry in touchdown conditions, inducing an undesired net lateral motion. The development of a robust control scheme to more effectively coordinate the legs should help mitigate these problems.

B.3 Results with force-maximizing control

Figure 8B shows the effects of switching to a max-force based control scheme on the performance of the simulated climber.

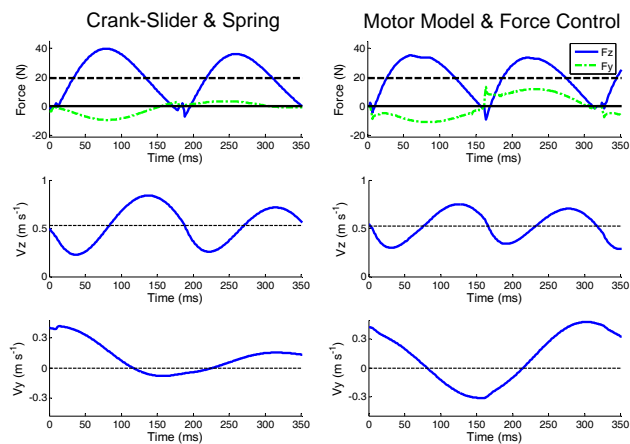


Fig. 8. Force, vertical velocity, lateral velocity, foot fall patterns, and speed for the original template model, the scaled version, and with the final proposed force-based control scheme.

A comparison of the dynamics reveals that the force-based case has some subtle differences from the previous template versions. The slopes of the force loading and unloading curves are different and more significantly the overall stride frequency is higher. The switch from a trajectory-tracking to a force-based control scheme releases our control of the resulting actuation frequency. While this frequency shifting during climbing can increase the performance of robot, it also complicates the dynamic coupling between the leg switching, body rotation, and the wrist-spring extension. While this could

alter the motion and efficiency of the model, the simulation results suggest that for the motor model chosen the resulting steady-state trajectories work well. In any case, the transients of the dynamics are an additional factor to consider when designing the controller.

The net result, however, is a realistically sized and powered dynamic climber that is very close to the template derived from animal studies. The overall projected speeds of 0.55 m/s compare very favorably to those of the scaled template (0.60 m/s). Some changes to the structure and actuation scheme are necessary, but the resulting performance is far superior to the ‘naive’ approaches discussed in Sec. IV.

The performance gain from switching to this type of controller is, however, less than that predicted from the earlier study of a one-dimensional climber. This is due in part to the sub-optimal leg coordination scheme implemented. The low gear ratio motor settings that the simple model predicts will give the best speeds often fail to synchronize in the 2D simulations. Another potential cause for the decreased performance is the braking that occurs just before leg transition. Currently this is due to a sub 50% duty factor and the details of the leg coordination scheme, but this deceleration at touchdown may also reflect the physical constraint associated with attaching the robot’s feet to the substrate.

VII. CONCLUSION AND FUTURE WORK

In general the simulation results are encouraging. The addition of a force-assist spring in parallel with the actuator in the legs and the switch to a force-maximizing control scheme should allow for a dynamic climber to climb at our target mass of 2kg. In addition it appears that the characteristic force and motion patterns of the animals and the steady gaits exhibited by the template should be reproducible in our anchored version. A preliminary CAD model of our proposed robot is shown in Fig. 9.

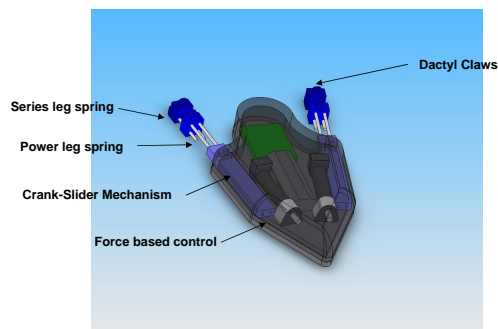


Fig. 9. Preliminary CAD model of proposed robot.

Furthermore, our scaling study suggests that this target size is about as large as this dynamic template can be instantiated with the current power density of motors, while preserving the percentage of mass of the

robot dedicated to actuators. Since absolute speed scales with the square root of length, or at the same rate at which the power/weight ratio must increase to preserve dynamic similarity, any increase in size will result in an under-powered robot. As shown in section IV, attempting to climb when underpowered has a severe effect on upward speed. Thus it appears that with our present power density this anchor represents the approximate upper limit on speed with this template.

Future theoretical work is required in the development of a robust leg synchronization scheme and in understanding how the structure and control scheme of the robot contribute to its lateral stability.

Once a robot has been built, additional future experimental work will need to be carried out including: investigating the effect of increased climbing speed on the attachment and detachment of feet, determining how to deal with pitch and roll without significant losses, and developing methods to deal with foot slippage or failed attachment.

Despite the significant amount of work remaining to transform this two-dimensional simulation into a three-dimensional climber, we believe that the results described here represent an encouraging step toward the development of a dynamic vertical climbing robot.

ACKNOWLEDGMENTS

The authors would like to Pei-Chun Lin for his help. This work was supported in part by DARPA/SPAWAR Contract N66001-05-C-8025. Jonathan Clark is supported by the IC Postdoctoral Fellow Program under grant number HM158204-1-2030.

REFERENCES

- [1] R. Blickhan and R. J. Full, "Similarity in multilegged locomotion: Bounding like a monopod," *Journal of Comparative Physiology*, vol. 173, no. 5, pp. 509–517, 1993.
- [2] G. A. Cavagna, N. C. Heglund, and Taylor C. R., "Mechanical work in terrestrial locomotion: Two basic mechanisms for minimizing energy expenditure," *American Journal of Physiology*, vol. 233, 1977.
- [3] T. A. McMahon and G. C. Cheng, "Mechanics of running. how does stiffness couple with speed?," *Journal of Biomechanics*, vol. 23, no. 1, pp. 65–78, 1990.
- [4] Marc H. Raibert, *Legged robots that balance*, MIT Press series in artificial intelligence. MIT Press, Cambridge, Mass., 1986.
- [5] R. Altendorfer, N. Moore, H. Komsuoglu, M. Buehler, Jr. Brown H. B., D. McMordie, U. Saranli, R. Full, and D. E. Koditschek, "Rhex: A biologically inspired hexapod runner," *Autonomous Robots*, vol. 11, no. 3, pp. 207–213, 2001.
- [6] J. G. Cham, S. A. Bailey, J. E. Clark, R. J. Full, and M. R. Cutkosky, "Fast and robust: Hexapedal robots via shape deposition manufacturing," *International Journal of Robotics Research*, vol. 21, no. 10, 2002.
- [7] C. Balaguer, A. Gimenez, J.M. Pastor, V.M. Padron, and C. Abderrahim, "A climbing autonomous robot for inspection applications in 3d complex environments.," *Robotica*, vol. 18, pp. 287–297, 2000.
- [8] G. La Rosa, M. Messina, G. Muscato, and R. Sinatra, "A low-cost lightweight climbing robot for the inspection of vertical surfaces.," *Mechatronics*, vol. 12, no. 1, pp. 71–96, 2002.
- [9] D. Bevely, S. Dubowsky, and C. Mavroidis, "A simplified cartesian-computed torque controller for highly geared systems and its application to an experimental climbing robot.," *Transactions of the ASME. Journal of Dynamic Systems, Measurement and Control*, vol. 122, no. 1, pp. 27–32, 2000.
- [10] T. Bretl, S. Rock, and J. C. Latombe, "Motion planning for a three-limbed climbing robot in vertical natural terrain," in *IEEE International Conference on Robotic and Automation (ICRA 2003)*, Taipei, Taiwan, 2003, vol. 205, pp. 2946 – 295.
- [11] "<http://www.vortexhc.com/vmrp.html>," .
- [12] J. Xiao, A. Sadegh, M. Elliot, A. Calle, A. Persad, and H. M. Chiu, "Design of mobile robots with wall climbing capability," in *Proceedings of IEEE AIM, Monterey, CA, Jul. 24-28, 2005*, pp. 438–443.
- [13] Daltorio K.A., Horchler A.D., Gorb S., Ritzmann R.E., and Quinn R.D., "A small wall-walking robot with compliant, adhesive feet," in *Proceedings of IROS, Edmonton, Canada*.
- [14] C. Menon, M. Murphy, and M. Sitti, "Gecko inspired surface climbing robots," in *Proceedings of IEEE ROBOT, Aug. 22-26, 2004*, pp. 431–436.
- [15] "<http://www.irobot.com>," .
- [16] K. Autumn, M. Buehler, M. R. Cutkosky, R. Fearing, R.J. Full, D. Goldman, R. Groff, W. Provancher, A. Rizzi, U. Saranli, A. Saunders, and D. Koditschek, "Robotics in scansorial environments," in *Unmanned Systems Technology VII*, D. W. Gage G. R. Gerhart, C. M. Shoemaker, Ed. SPIE, 2005, vol. 5804, pp. 291–302.
- [17] K. Autumn, S. T. Hsieh, D. M. Dudek, J. Chen, C. Chitaphan, and R. J. Full, "Dynamics of geckos running vertically," *Journal of Experimental Biology*, vol. 209, pp. 260–270, 2006.
- [18] D. I. Goldman, T. S. Chen, D. M. Dudek, and R. J. Full, "Dynamics of rapid vertical climbing in a cockroach reveals a template," *Journal of Experimental Biology*, vol. 209, pp. 2990–3000, 2006.
- [19] R. J. Full and K. Meijer, "Metrics of natural muscle," in *Electro Active Polymers (EAP) as Artificial Muscles, Reality Potential and Challenges*, Y. Bar-Cohen, Ed., pp. 67–83. 2001.
- [20] J. E. Clark and D. E. Koditschek, "A spring assisted one degree of freedom climbing model," in *Accepted for publication in Springer-Verlang's Lecture Notes on Control and Informatoin Sciences*, 2006, pp. 43–64.
- [21] R. McN. Alexander and A. S. Jayes, "A dynamic similarity hypothesis for the gaits of quadrupedal mammals," *Journal of Zoology*, vol. 201, pp. 135–152, 1983.
- [22] J. Schmitt, M. Garcia, R. Razo, P. Holmes, and R. J. Full, "Dynamics and stability of legged locomotion in the horizontal plane: a test case using insects.," *Biological Cybernetics*, vol. 86, no. 5, pp. 343–53, 2002.
- [23] R. McN. Alexander, *Principles of Animal Locomotion*, Princeton University Press, 2003.
- [24] R. McN. Alexander, *Elastic Mechanisms in Animal Movement*, Cambridge: Cambridge University Press, 1988.
- [25] H. M. Herr, G. T. Huang, and T. A. McMahon, "A model of scale effects in mammalian quadrupedal running," *The Journal of Experimental Biology*, vol. 205, pp. 959–967, 2002.
- [26] J. M. Hollerbach, I. W. Hunter, and J. Ballantyne, "A comparative analysis of actuator technologies for robotics," in *The Robotics Review 2*, pp. 299–342. The MIT Press, 1992.
- [27] S. Kim, J. E. Clark, and M. R. Cutkosky, "isprawl: Autonomy, and the effects of power transmission," in *International Conference on Climbing and Walking Robots (CLAWAR)*, vol. 7. Professional Engineering Publishing, Madrid, Spain, 2004.
- [28] M.J. Boggess, R.T. Schroer, R.D. Quinn, and R.E. Ritzmann, "Mechanized cockroach footpaths enable cockroach-like mobility," in *Proceedings of IEEE ICRA, New Orleans, LA, 2004*.
- [29] "<http://www.maxonmotorusa.com>," .
- [30] Haldun Komsuoglu, *Toward a formal framework for open-loop stabilization of rhythmic tasks*, Ph.D. thesis, University of Michigan, 2004.
- [31] S. Kim, A. Asbeck, M. R. Cutkosky, and W. R. Provancher, "Spinybot ii: Climbing hard walls with compliant microspines," in *Proceedings, IEEE - ICAR, Seattle, WA, July 17-20, 2005*.
- [32] M. Spenko, M. R. Cutkosky, R. Majidi, R. Fearing, R. Groff, and K. Autumn, "Foot design and integration for bioinspired climbing robots," in *In review for Unmanned Systems Technology VIII*. SPIE, 2006.
- [33] E. Klavins and D. E. Koditschek, "Phase regulation of decentralized cyclic robotic systems," *International Journal of Robotics Reserach*, vol. 21, no. 3, pp. 257–275, 2002.